GaN HEMT Thermal Characteristics Evaluation Using an Integrated Approach Based on the Combined Use of First-Principles and Device Simulations

Maryia Baranava, Dzmitry Hvazdouski Vladislav Volcheck, Viktor Stempitsky
Belarusian State University of Informatics and Radioelectronics
Minsk, Belarus
vstem@bsuir.by

Dao Dinh Ha, Trung Tran Tuan
Le Quy Don Technical University
Hanoi, Vietnam
havixuly@gmail.com

***Abstract*—The GaN high electron mobility transistor (HEMT) thermal characteristics were evaluated employing an integrated approach based on the combined use of *ab initio* (first-principles) and device simulations. The necessity of utilizing such a method arises when model parameters required for device simulation are unavailable or not suited to certain conditions. A fine example is thermal conductivity of crystalline materials, which is strongly dependent on the defect density, isotopic purity and temperature. Since the developed temperature due to self-heating is highly sensitive to the thermal conductivities of certain regions of the device structure, it is of great importance to use correct thermal conductivity models that are incorporated into the heat flow equation. A combination of *ab initio* calculations and solutions of the linearized phonon Boltzmann transport equation is a high-end tool to estimate the thermal properties of crystalline materials. In this paper, firstly, the values of the thermal conductivity and thermal capacity of AlN, GaN, $Al_{0.21}Ga_{0.79}N$ and $Al_{0.5}Ga_{0.5}N$ were calculated in the range of temperature from 20 K to 1000 K. Secondly, device simulation of a GaN HEMT was performed and the thermal characteristics were evaluated.**

I. Introduction

Since 1980, the high electron mobility transistor (HEMT) technology has continued to achieve widespread use and drive innovation in the field of information and communications. Able to allow for low-noise performance at frequencies up to the millimeter wave band, HEMTs are used in a wide variety of applications, including satellite broadcasting receivers, mobile phones, radar systems, navigation systems, voltage converters and low-power amplifiers. Further, research and development activities undertaken by corporations and governments directed at improving and commercializing the novel technology are becoming extremely active throughout the world. In addition to standard GaAs-based HEMTs, the development of ultra-high-frequency InP and low-power/high-frequency GaN devices is advancing at a fast pace. Going forward, HEMTs are expected to be featured in the fifth-generation millimeter wave mobile network technology [1].

The HEMT, named alternatively as the modulation-doped or heterostructure field-effect transistor, is a field-effect transistor exploiting the high in-plane mobility of electrons in the channel formed along a semiconductor heterojunction. In recent years, device engineers have greatly focused on the development of AlGaN/GaN HEMT. The immense interest in the AlGaN/GaN heterojunction stems from several factors. First, the wide band gap of GaN yields a high breakdown voltage, which enables high-power operation. Also, the saturation velocity of electrons in GaN is over a factor of two larger than that in silicon, which is valuable for high-frequency operation. Moreover, a very high electron concentration is induced by polarization at the AlGaN/GaN interface, providing a large current density. At the same time, the AlGaN/GaN HEMT is characterized by a temperature rise and a non-uniform distribution of the dissipated heat power that lead to the formation of a hot spot at the active area of the device and result in the degradation of the drain current and the output power [2]. In order to mitigate the self-heating effect, a variety of thermal management solutions have been proposed: atomic bonding of the AlGaN/GaN epitaxial structure to a chemical vapor deposition nanocrystalline diamond layer after the silicon substrate is etched away [3]; direct growth of the AlGaN/GaN structure on a diamond substrate by metalorganic vapor-phase epitaxy [4]; backside filling of the through trench, etched locally in the silicon substrate, by an AlN and copper combination [5]; integration of heat spreading elements formed by a material with a high thermal conductivity, for example, diamond [6] and graphene [7], into the transistor structure.

Controlling the temperature is critical to the efficiency and reliability of many electronic devices and circuitry. Thermal simulation, widely recognized as a crucial aspect of computer-aided design, can assist in thermal management by enabling engineers to identify the root cause of thermal problems and evaluate a wide range of alternative variants to optimize the design. Thermal conductivity is one of the input parameters of the heat flow equation [8] and, in case of crystalline materials, is strongly dependent on the defect density, isotopic purity and temperature [9]. This is critical to take into account during simulation, as the developed temperature due to self-heating is very sensitive to the thermal conductivities of certain areas of the device structure. Otherwise, a significant error will occur. Thus, it is important to use appropriate thermal conductivity models that are incorporated into the heat flow equation. The

empirical values of the thermal conductivity of GaN and AlN reported so far vary considerably, which are mainly attributed to the difference in the purity and microstructure of the samples studied. In comparison with the binary compounds, the thermal transport in the ternary alloys is even more complicated due to the effect of alloy scattering, which is shown to dominate [10]. In fact, only few works deal with the thermal conductivity of AlGaN [10–13]. A combination of *ab initio* (first-principles) calculations and solutions of the linearized phonon Boltzmann transport equation is a powerful tool to estimate the thermal properties of crystalline materials. In this paper, we calculated the values of the thermal conductivity and thermal capacity of AlN, GaN, $Al_{0.21}Ga_{0.79}N$ and $Al_{0.5}Ga_{0.5}N$ in the range of temperature from 20 K to 1000 K and evaluated the thermal characteristics of a GaN HEMT in the framework of our integrated approach based on the consecutive usage of first-principles and device simulations. However, we have not had yet a possibility to make measurements to prove our findings.

In Section II, the underlying principle of the approach used in this work is explained. Section III contains the information about the details of the first-principles and device simulations, the electrical and thermal characteristics of the GaN HEMT.

II. Integrated Approach Based on First-Principles and Device Simulations

The rapid development of micro- and nanoelectronics is related with the design and discovery of new materials, which may either be a structural modification of a previously known material (such as graphite and graphene [14]), or an unknown combination of an atomic composition and a symmetry group, or a heterostructure, in which the energy influence between the materials is significant. The development of novel technologies based on advanced materials paves the way for the creation of new applications. In order to make a new material available for device simulation, its basic parameters must be determined and verified. The basic parameters have a primary influence on the processes of generation/recombination and transport of charge carriers, and, as a result, define the density and mobility of the two-dimensional electron gas realized in GaN HEMTs.

For example, the simulation of a device structure based on quasi-two-dimensional films requires a preliminary determination of a minimum set of parameters. Band gap of the material, electron affinity, density of states for electrons and holes, dielectric constant of the material, effective mass and carrier mobility this is a necessary minimum for device simulation. Novel quasi-two-dimensional materials are not always well studied experimentally.

It may also be necessary to determine some charge carrier recombination parameters. These parameters, describing the physical properties of quasi-two-dimensional films, are not integrated into the software packages of device simulation. It is possible to obtain the values of some parameters without involving experimental methods using, instead, calculations from first principles [15, 16]. In accordance with the proposed approach, a set of parameters determined by first-principles calculations is used at the stage of technology computer-aided design (TCAD) simulation (Fig.1).

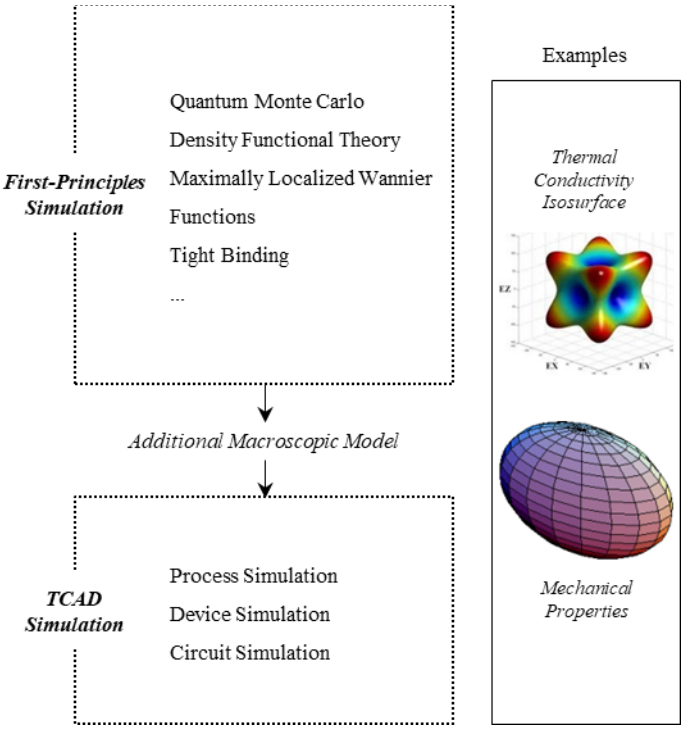

Fig. 1. Scheme of the integrated approach based on the combined use of first-principles and TCAD simulations

The first-principles simulation is to carry out calculations in order to obtain data on the fundamental properties of crystals, molecules, and other nanoscale objects without invoking experimental data. The implementation of this simulation is possible thanks to the such fundamental equation of quantum mechanics as the Schrodinger equation. The problem of solving the many-particle Schrodinger equation lies in a very large number of variables. For example, five electrons in a 10×10×10 grid require 10 Petabytes of memory.

Traditional methods for determining the electronic structure, in particular, the Hartree-Fock method and based them, describe the system using a multi-electron wave function. The electron density theory (DFT) is the solution to this problem [17]. The main goal of the DFT is to replace the multi-electron wave function with the electron density in the description of the electron subsystem. This leads to a significant simplification of the problem, since the manyelectron wave function depends on $3N$ variables – 3 spatial coordinates for each of the N electrons, and the density is a function of only three spatial coordinates.

The results of first-principle simulation can be used in fundamental models (e.g., a thermal conductivity model or magnetic models) to obtain macroscopic parameters. For example, the exchange interaction integral and other magnetic parameters can be determined by obtaining data of the crystal lattice total energy in several established magnetic states [18]. This can be used to simulation of magnetic devices. In the case of using the thermal conductivity model, the phonon spectrum will be determined at the initial stage. Further, the coefficient of thermal conductivity or heat capacity coefficient are easy to obtain. These results can be used by TCAD simulation software. The results of this integrated approach are presented below.

T18M-108 and 19-7009 of Belarusian Republican Foundation for Fundamental Research

The description of physical processes in the device structure is based on the use of the standard equations for TCAD simulation: Poisson, continuity, carrier transport (diffusion-drift model, energy balance model, hydrodynamic model). At the same time, numerous models that are part of the instrumentation and technology modeling software systems serve to describe specific physical processes and phenomena. Some of them require adaptation and calibration, taking into account the characteristics of physical processes in the considered instrument structures by using methods for determining the significance of parameters and optimization methods.

III. GaN HEMT Thermal Characteristics Evaluation

The sequence of the steps performed to evaluate the thermal characteristics of the GaN HEMT is given in Fig. 2.

A. First-Principles Simulation

At the first stage, the first-principles calculation (ab initio simulation as it is commonly in literature) is carried out using the VASP software package recognized as a common standard for the study of the fundamental properties of crystalline materials [19]. VASP is developed for the simulation of atomic scale materials, e.g. electronic structure calculations and quantum mechanical molecular dynamics using projector-augmented-wave method and a plane wave basis set. The principal methodology is DFT. With the help of VASP, the structural and electronic properties, the energy and the stress of the AlN, GaN and $Al_{0.5}Ga_{0.5}N$ systems are obtained.

For verification, the fundamental physical parameters (structural and electronic properties) are compared with the experimental ones. The condition for recognizing the method correct, that is, providing realistic simulation: the structural characteristics differ from experimental ones by no more than 5% (in particular, the lattice constants). In the results, the structural properties of supercell as well as the force constant data are obtained with a set of tags of simulations that satisfy the condition above.

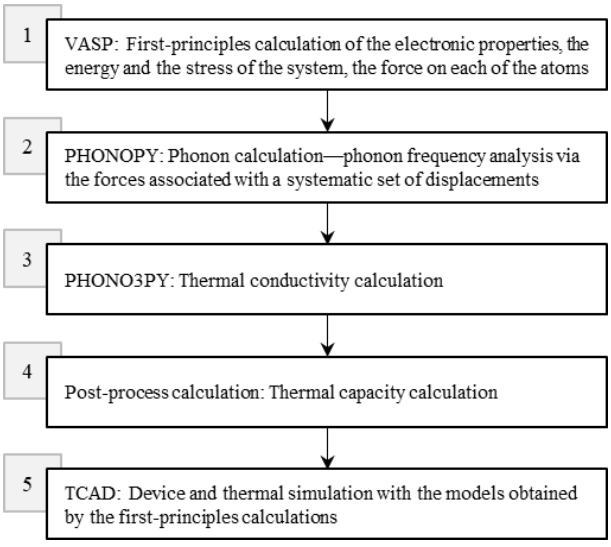

Fig. 2. Scheme of the integrated approach used to evaluate the GaN HEMT thermal characteristics

At the second stage, the phonon properties are calculated using the PHONOPY code. The information of the phonon frequency is necessary for accounting the thermal properties of crystalline materials. PHONOPY is an open source package for phonon calculations at harmonic and quasi-harmonic [20, 21]. When an atom in a crystal is displaced from its equilibrium position, the forces on each of the atoms in the crystal are increased. The analysis of the forces associated with a systematic set of displacements provides a series of the phonon frequencies. First-principles phonon calculations with FDM [22] can be made in this way. At the conclusion of this stage, a set of phonon frequencies for the structures under study are obtained.

The thermal conductivity calculation is carried out at the next stage. PHONO3PY is another open source package developed for the phonon-phonon interaction and thermal conductivity calculations. This software calculates the phonon–phonon interaction and related properties using the supercell approach (The supercell consists of unit cells that describe the same crystal. Many methods that use a supercell perturbate it somehow to determine properties which cannot be determined by the initial cell, e.g. during phonon calculations). The linearized phonon Boltzmann equation is calculated on this stage [23]. In the results, sets of the temperature dependence of the thermal conductivity are obtained.

The thermal conductivity is calculated by the PHONO3PY package. The phonon-phonon interaction calculation using the supercell approach and the method based on the linearized phonon Boltzmann transport equation with single-mode RTA are implemented. In RTA, the thermal conductivity is written in a closed form:

$$\lambda = \frac{1}{NV_0}\sum_{\lambda} C_\lambda v_\lambda \otimes v_\lambda \tau_\lambda, \tag{1}$$

where N and V_0 are the number of the unit cell in the system and the volume of the unit cell, respectively.

The suffix λ represents the phonon mode as the pair of phonon wave vector q and branch j, $\lambda \equiv (q, j)$, and similarly we denote $-\lambda \equiv (-q, j)$. C_λ is the mode heat capacity given as

$$C_\lambda = \kappa\left(\frac{\hbar\omega_\lambda}{\kappa T}\right)^2 \frac{\exp\left(\frac{\hbar\omega_\lambda}{\kappa T}\right)}{\left(\exp\left(\frac{\hbar\omega_\lambda}{\kappa T}\right)-1\right)^2}, \tag{2}$$

where κ is the Boltzmann constant, $\hbar$ is the reduced Planck constant, T is the temperature, $\omega_\lambda = \omega(q, j)$ is the phonon frequency.

In (1):

$$v_\lambda = \nabla_q \omega(q, j), \tag{3}$$

where τ_λ is the single-mode relaxation time.

We performed a series of calculations against different exchange correlation potentials and convergence criteria. After these examinations, we chose the calculation settings described

which are considered to give results accurate enough for our discussion.

B. Thermal Conductivity and Thermal Capacity

The temperature dependence of the thermal conductivities of AlN, GaN, $Al_{0.21}Ga_{0.79}N$ and $Al_{0.5}Ga_{0.5}N$ is shown in Fig. 3.

The thermal capacities are calculated on the basis of the respective thermal conductivity results. The dependence of the thermal capacities of AlN, GaN, $Al_{0.21}Ga_{0.79}N$ and $Al_{0.5}Ga_{0.5}N$ on temperature is shown in Fig. 4.

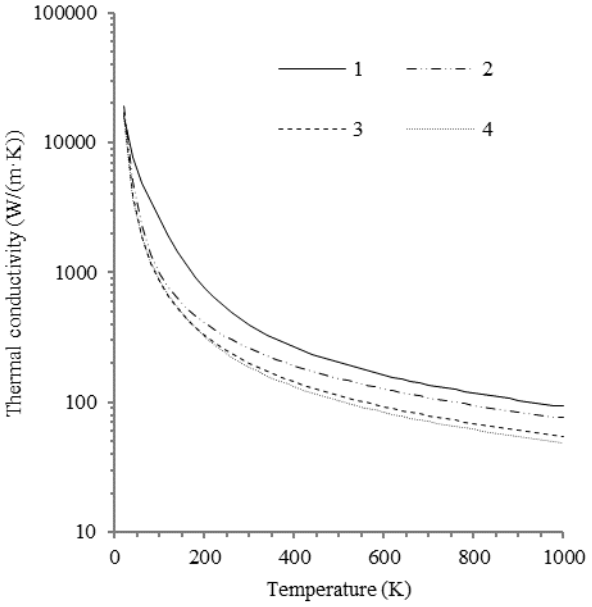

Fig. 3. Temperature dependence of the thermal conductivity of AlN (1), GaN (2), $Al_{0.21}Ga_{0.79}N$ (3) and $Al_{0.5}Ga_{0.5}N$ (4)

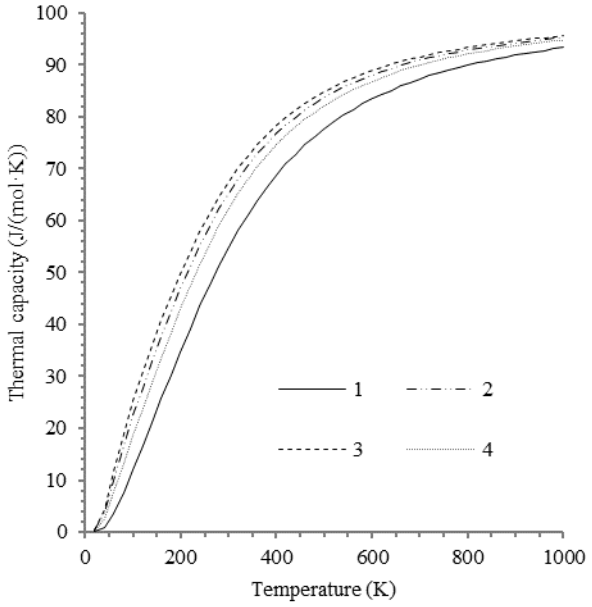

Fig. 4. Temperature dependence of the thermal capacity of AlN (1), GaN (2), $Al_{0.21}Ga_{0.79}N$ (3) and $Al_{0.5}Ga_{0.5}N$ (4)

The values of the thermal conductivity obtained by the first-principles simulation for pure AlN and GaN agree well with the experimental data provided in [10]. This confirms the validity of the methods applied in our work.

After the thermal parameters of GaN and $Al_{0.21}Ga_{0.79}N$ are calculated, they are transferred to the device simulation stage.

C. Device Simulation

A two-dimensional schematic representation of the GaN HEMT is given in Fig. 5. The heterostructure consists of a 20 nm $Al_{0.21}Ga_{0.79}N$ barrier layer and a 1.5 μm GaN buffer layer. In order to emphasize the importance of choosing a suitable thermal conductivity model, GaN is defined as the substrate material. The gate length equals to 0.5 μm. The source-to-gate and gate-to-drain distances are 1 μm and 2.5 μm, respectively. The gate width is 100 μm.

The device simulation is performed in the framework of the drift-diffusion theory with the Farahmand mobility model [24]. In order to incorporate the self-heating effect into the simulation, the heat flow equation is solved self-consistently with the basic semiconductor equations [8]. The thermal conductivity of GaN in the temperature range from 300 K to 600 K can be fitted by the formula:

$$\lambda(\mathrm{GaN}) = 258\left(\frac{T}{300}\right)^{-1.03}. \qquad (4)$$

As opposed to our results, in order to make a comparison, the following model [25] is also used:

$$\lambda(\mathrm{GaN}) = 130\left(\frac{T}{300}\right)^{-0.28}. \qquad (5)$$

In Fig. 6, the dependences of the drain current and the maximum temperature developed by the device on the drain voltage (V_d) are presented. As seen from the chart, at V_d = 10 V, the drain current equals to 0.076 A and 0.059 A when (4) and (5) are used, respectively. The respective maximum temperatures are 436 K and 483 K.

In Fig. 7, the temperature distribution profiles across the substrate built under the center of the gate at V_d = 10 V is presented. Owing to the higher thermal conductivity of GaN provided by our model, the temperature difference between the top and the bottom of the substrate is 134 K, as opposed to the value of 181 K calculated with (5).

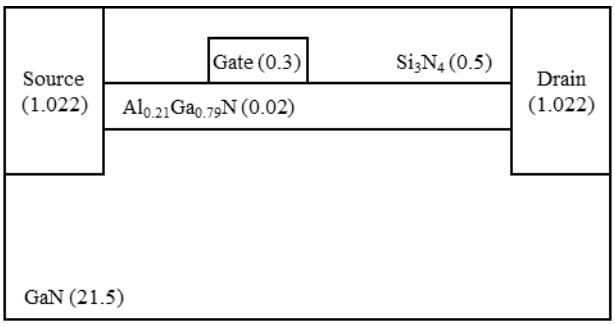

Fig. 5. GaN HEMT device structure (in brackets, the thickness values in microns are indicated)

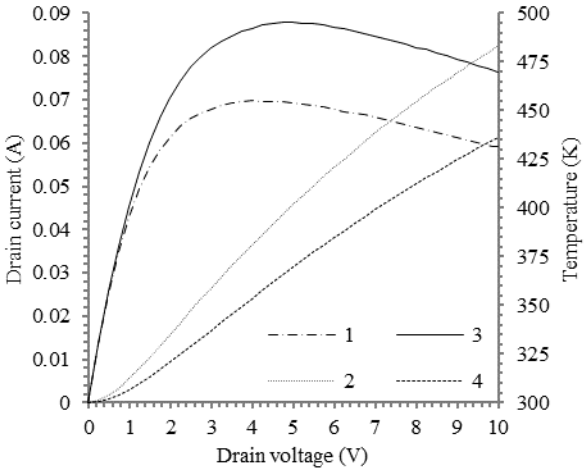

Fig. 6. Dependences of the drain current (1 and 3) and the maximum temperature (2 and 4) on the drain voltage: 1 and 2 are calculated using (5), while 3 and 4 are obtained using our model

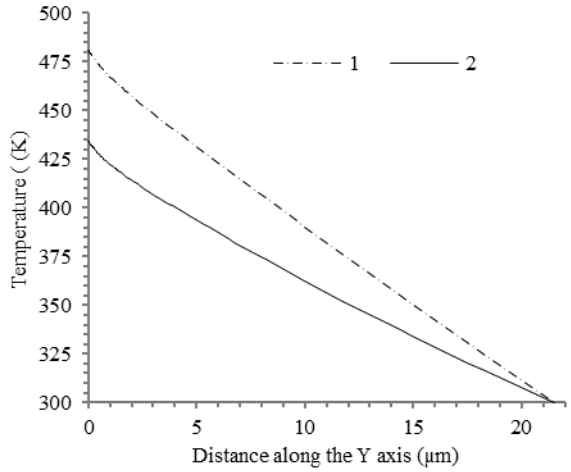

Fig. 7. Temperature distribution profile across the substrate: 1 is calculated using (5) and 2 is obtained using our model

CONCLUSIONS

We proposed and verified an integrated approach based on the combined use of first-principles and device simulations to evaluate the thermal characteristics of a GaN HEMT. The values of the thermal conductivity and thermal capacity of AlN, GaN, $Al_{0.21}Ga_{0.79}N$ and $Al_{0.5}Ga_{0.5}N$ were calculated in the range of temperature from 20 K to 1000 K. The thermal conductivities of pure AlN and GaN are in good agreement with the experimental data. The thermal characteristics of a GaN HEMT on the GaN substrate were simulated and the importance of choosing a suitable thermal conductivity model was shown.

REFERENCES

[1] T. Mimura, "Invention of high electron mobility transistor (HEMT) and contributions to information and communications field," Fujitsu Sci. Tech. J., vol. 54, pp. 3–8, October 2018.

[2] Z. Yan, G. Liu, J. M. Khan, and A. Balandin, "Graphene quilts for thermal management of high-power GaN transistors," Nat. Commun., vol. 3, pp. 1–8, May 2012.

[3] J. G. Felbinger et al., "Comparison of GaN HEMTs on diamond and SiC substrates," IEEE Electron Device Lett., vol. 28, pp. 948–950, November 2007.

[4] K. Hirama, Y. Taniyasu, and M. Kasu, "AlGaN/GaN high-electron mobility transistors with low thermal resistance grown on single-crystal diamond (111) substrates by metalorganic vapor-phase epitaxy," Appl. Phys. Lett., vol. 98, pp. 162112-1–162112-3, April 2011.

[5] G. Pavlidis et al., "The effects of AlN and copper back side deposition on the performance of etched back GaN/Si HEMTs," IEEE Electron Device Lett., vol. 40, pp. 1060–1063, July 2019.

[6] K. S. Grishakov, V. F. Elesin, N. I. Kargin, R. V. Ryzhuk, and S. V. Minnebaev, "Effect of diamond heat spreader on the characteristics of gallium nitride-based transistors," Russ. Microelectron., vol. 45, pp. 41–53, 2016.

[7] V. S. Volcheck, I. Yu. Lovshenko, V. T. Shandarovich, and D. H. Dao, "Gallium nitride high electron mobility transistor with an effective graphene-based heat removal system," Doklady BGUIR, vol. 18, pp. 72–80, 2020.

[8] G. H. Wachutka, "Rigorous thermodynamic treatment of heat generation and conduction in semiconductor device modeling," IEEE Trans. Comput.-Aided Des., vol. 9, pp. 1141–1149, November 1990.

[9] L. Lindsay, D. A. Broido, and T. L. Reinecke, "Thermal conductivity and large isotope effect in GaN from first principles," Phys. Rev. Lett., vol. 109, pp. 095901-1–095901-5, August 2012.

[10] M. Slomski, L. Liu, J. F. Muth, and T. Paskova, "Growth technology for GaN and AlN bulk substrates and templates," in Handbook of GaN semiconductor materials and devices, W. Bi, H.-C. Kuo, P.-C. Ku, and B. Shen, Eds. New York: CRC Press, 2018, pp. 143–167.

[11] B. C. Daly, H. J. Maris, A. V. Nurmikko, M. Kuball, and J. Han, "Optical pump-and-probe measurement of the thermal conducvitity of nitride thin films," J. Appl. Phys., vol. 92, pp. 3820–3824, October 2002.

[12] W. Liu and A. A. Balandin, "Temperature dependence of thermal conductivity of $Al_xGa_{1-x}N$ thin films measured by the differential 3ω technique," Appl. Phys. Lett., vol. 85, pp. 5230–5232, November 2004.

[13] S. Adachi, "Lattice thermal conductivity of group-IV and III-V semiconductor alloys," J. Appl. Phys., vol. 102, pp. 063502-1–063502-7, September 2007.

[14] K. S. Novoselov et al., "A roadmap for graphene," Nature, vol. 490, pp. 192–200, October 2012.

[15] C. R. Dean et al., "Boron nitride substrates for high-quality graphene electronics," Nature Nanotech., vol. 5, pp. 722–726, August 2010.

[16] P. Avouris, "Graphene: Electronic and photonic properties and devices," Nano Lett., vol. 10, pp. 4285–4294, September 2010.

[17] R. G. Parr, "Density-functional theory of atoms and molecules," Horizons of Quantum Chemistry, vol. 3, pp. 5–15, November 1980.

[18] M. S. Baranava, D. C. Hvazdouski, V. A. Skachkova, V. R. Stempitsky, and A. L. Danilyuk, "Magnetic interactions in $Cr_2Ge_2Te_6$ and $Cr_2Si_2Te_6$ monolayers: ab initio study," Materials Today: Proceedings, vol. 20, p. 3, pp. 342–347, 2020.

[19] G. Kresse, M. Marsman, and J. Furthmuller, "VASP The Guide: Tutorial," Vienna: University of Vienna, 2014, Available: https://www.vasp.at.

[20] A. Katre, A. Togo, I. Tanaka, and G. K. H. Madsen, "First principles study of thermal conductivity cross-over in nanostructured zinc chalcogenides," J. Appl. Phys., vol. 117, pp. 045102-1–045102-6, January 2015.

[21] Y. Ikeda, A. Seko, A. Togo, and I. Tanaka, "Phonon softening in paramagnetic bcc Fe and its relationship to the pressure-induced phase transition," Phys. Rev. B, vol. 90, pp. 134106-1–134106-7, October 2014.

[22] K. Parlinski, Z. Q. Li, and Y. Kawazoe, "First-principles determination of the soft mode in cubic ZrO2," Phys. Rev. Lett., vol. 78, pp. 4063–4066, January 1997.

[23] L. Chaput, "Direct solution to the linearized phonon Boltzmann equation," Phys. Rev. Lett., vol. 110, pp. 265506-1–265506-5, June 2013.

[24] M. Farahmand et al., "Monte Carlo simulation of electron transport in the III-nitride wurtzite phase materials system: binaries and ternaries," IEEE Trans. Electron Devices, vol. 48, pp. 535–542, March 2001.

[25] J. Piprek, Semiconductor Optoelctronic Devices: Introduction to Physics and Simulation. San Diego, CA: Academic Press, 2003.